

## THE EXTENDED CELLULAR AUTOMATON (X-CA) MODEL FOR SOLAR FLARES

H. Isliker<sup>1</sup>, A. Anastasiadis<sup>2</sup>, and L. Vlahos<sup>1</sup>

<sup>1</sup> Department of Physics, University of Thessaloniki, 54124 Thessaloniki, GREECE

<sup>2</sup> National Observatory of Athens, Institute for Space Applications and Remote Sensing, 152 36 Penteli, GREECE

### ABSTRACT

We have developed a new type of cellular automaton (CA) model, the *extended CA (X-CA)*, for the study of solar flares. The X-CA model is consistent with the MHD approach, in contrast to the previously proposed CA models (classical CAs), it consistently yields all the relevant physical variables, and it successfully reproduces the observed distributions of total energy, peak flux, and duration of solar flares. We present and discuss the relevant plasma processes and set-up which are implemented by the X-CA model in the framework of a commonly accepted solar flare scenario.

Key words: Sun; flares; Cellular Automata; Self Organized Criticality.

### 1. INTRODUCTION

It is now widely accepted that the solar activity is mainly due to the dissipation of the magnetic energy stored previously in the solar corona. Magnetic energy release manifests itself in a large variety of phenomena, ranging from heating to solar flares. Observations of the radiation signatures of solar energetic particles (especially in the hard X-rays) indicate that the energy release process is fragmented into a large number of sub-events (Vilmer 1993; Trotter 1994; Aschwanden et al. 1995, Vilmer and Trotter 1997). In the last two decades, the availability of several space-born solar instruments, together with the existence of several ground based telescopes, have given the opportunity to perform a number of statistical studies of the flaring activity of the Sun. These types of observations (Dennis 1985; Vilmer 1987; Pick et al. 1990; Crosby et al. 1993; Crosby et al. 1998) revealed that the frequency-distributions of flares as a function of total energy, peak luminosity, and duration are well-defined power laws, extending over several orders of magnitude.

Traditionally, the study of the energy release process was relying on the magnetohydrodynamic (MHD) theory. In this framework, the most common approach was the development of numerical simulation codes, given the complex nature of the energy release problem in the solar

corona, which involves strongly nonlinear effects (e.g. Einaudi et al. 1996; Georgoulis et al. 1998, and references therein). In MHD numerical simulations, the energy release process (i.e. magnetic reconnection) is simulated in detail, but these simulations are time consuming and can only treat a small number of reconnection events (bursts) and relatively small volumes, leading thus to poor statistics for comparison to solar flare observations.

Alternatively, several cellular automaton (CA) models, based on the approach used in complex dynamical system theory, have been developed in order to explain the solar flare statistics derived from the observations (Lu and Hamilton 1991; Lu et al. 1993; Vlahos et al. 1995; Galsgaard 1996; Georgoulis and Vlahos 1996; 1998, Georgoulis et al. 2001). We will term these models *classical CA models*. The classical CA models simulate the energy storage/release process using simple evolution rules, neglecting the details of the processes. These models allow the global modeling of solar active regions, at the expense of understanding in details the underlying physics. The main advantage of them is that they can treat a large number of elementary energy-release events and relatively large volumes, yielding thus results on a good statistical ground, and that they can explain the power-law frequency distributions of the solar flare parameters.

### 2. DESCRIPTION OF THE X-CA MODEL

In our previous work (Isliker et al. 1998), we tried to solve the problem of the vague association of the classical CA model's components with physical variables and processes, which was their most important disadvantage. Our goal was to give a physical interpretation to the classical CAs and to try to connect the two complementary approaches (MHD and CA) for the solar flare problem. Our study revealed the role of several components of the classical CA models, such as the possible physical interpretations of the grid-variable, the physical meaning of the time step and of the spatial discreteness, the nature of the energy release process, and the role of the diffusivity. On the other hand, several unsatisfying properties of the classical CA models have been found, such as inconsistencies with the MHD equations (e.g.  $\nabla \mathbf{B}$  is uncontrolled), and the non-availability of secondary variables

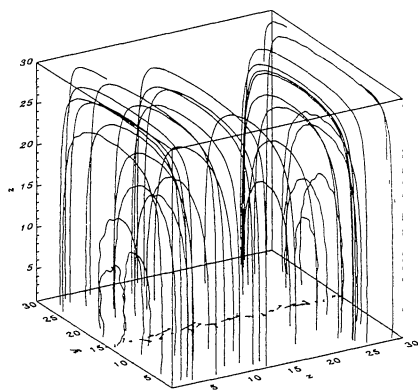


Figure 1. The magnetic topology of the X-CA model, together with a subset of the current vectors

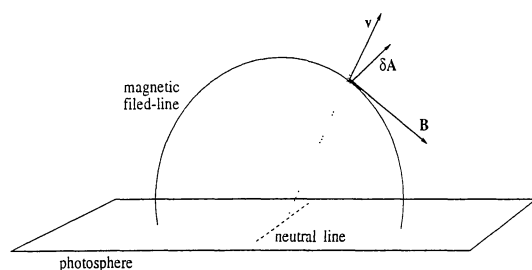


Figure 2. Sketch to illustrate the loading process: the loading increments  $\delta\mathbf{A}$  can be considered as being proportional to  $\mathbf{v} \times \mathbf{A}$ , with  $\mathbf{v}$  the velocity of the implicitly assumed plasma, and  $\mathbf{B}$  the magnetic field.

(current density  $\mathbf{J}$ , electric field  $\mathbf{E}$ ). In order to overcome these problems, we have constructed a new class of CA models for solar flares, termed *extended CA* (X-CA) model (Isliker et al. 2000, 2001), which are compatible with MHD and yield statistical results that are compatible with the observations.

The X-CA model consists in the combination of a classical CA model with a set-up which is super-imposed onto the classical CA (for details see Isliker et al. 2000, 2001): We use a 3-D cubic grid ( $30 \times 30 \times 30$  in the following) with the vector potential  $\mathbf{A}$  as the primary grid variable. The central problem is how to calculate derivatives, since CAs are by their nature discrete models, as demonstrated in Isliker et al. (1998). We differentiate  $\mathbf{A}$  and the magnetic field  $\mathbf{B}$  by using 3-D cubic spline interpolation (evaluating several alternative methods, it turned out that calculating the derivatives in this way has remarkable advantages over other methods). The magnetic field  $\mathbf{B}$  and the current density  $\mathbf{J}$  are then given as secondary variables, as in MHD, and determined according to Maxwell's equations,

$$\mathbf{B} = \nabla \times \mathbf{A} \quad (1)$$

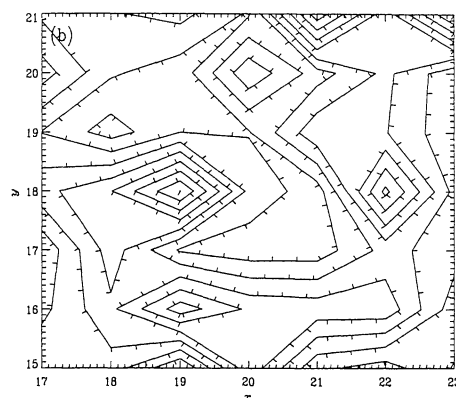
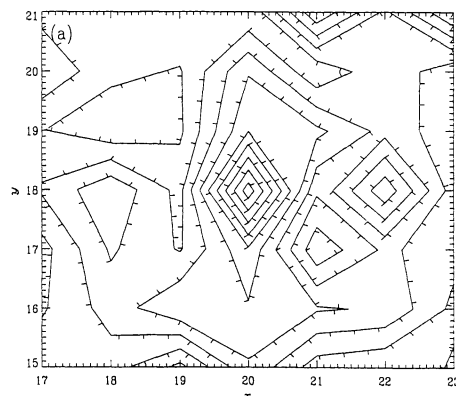


Figure 3. Contour-plot of the current-density, before (top), and after (bottom) a burst, which occurs in the middle of the plot (the  $z$ -coordinate is fixed)

(which ensures that  $\nabla \cdot \mathbf{B} = 0$ ), and

$$\mathbf{J} = \frac{c}{4\pi} \nabla \times \mathbf{B}. \quad (2)$$

The electric field is determined by the simple Ohm's law,

$$\mathbf{E} = \eta \mathbf{J}. \quad (3)$$

The dynamic evolution of the X-CA has two distinct phases. In the loading phase, random field increments  $\delta\mathbf{A}$  are dropped at random sites. If a local instability criterion is fulfilled, local bursts (relaxing redistributions of  $\mathbf{A}$ ) are triggered, during which energy is released, whose amount is determined as Ohmic dissipation ( $\sim \eta \mathbf{J}^2$ ).

As a critical quantity either  $d\mathbf{A}$ , the stress in  $\mathbf{A}$ , as defined in the classical CAs (e.g. Lu & Hamilton 1991), or, new in the context of CAs, the current density  $\mathbf{J}$  is used.

## 3. RESULTS AND CONCLUSIONS

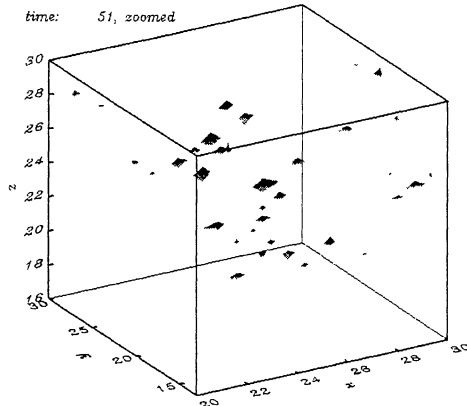


Figure 4. Current dissipation regions (i.e. volumes enclosing regions of super-critical current) at a temporal snap-shot during a flare

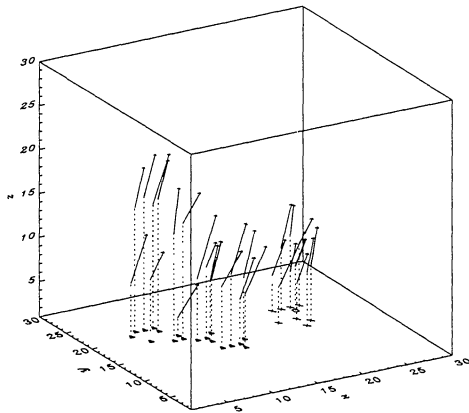


Figure 5. The electric field-vectors during a flare, at three different time-steps: at the beginning of the flare (bold-vector, projected grid-site in  $x$ - $y$ -plane marked with a rectangle); after nine time-step (marked with 'x'); after 91 time-steps (marked with triangles). The vectors are shown in 3-D parallel projection, rescaled for visualization purposes, with length proportional to  $|\mathbf{E}|$ . Note that the electric fields of three different time-steps are shown together for visualization purposes, in the model actually only one set appears at a time, the fields of the previous time-steps have become zero again, at later times.

The X-CA model yields power-law frequency distributions for the diverse flare parameters (total energy, peak flux) which are compatible with the observations, and, unlike the classical CAs, the X-CA yields insight into the physical scenario and the physical processes during flares:

1. The vector-potential, magnetic field, and current exhibit large-scale organization and quasi-symmetries. Depending on the directionality of loading and the boundary conditions, the global topology of the magnetic field has two varieties: Either it forms an arcade of magnetic field lines (Fig. 1), or it forms closed magnetic field lines around and along a neutral line.

2. The temporal evolution of the model follows the MHD induction equation, which, expressed in terms of the vector potential, writes

$$\frac{\partial \mathbf{A}}{\partial t} = \mathbf{v} \wedge \mathbf{B} + \eta \frac{c^2}{4\pi} \nabla^2 \mathbf{A} - \eta \frac{c^2}{4\pi} \nabla(\nabla \cdot \mathbf{A}) + \nabla \chi, \quad (4)$$

where  $\eta$  is the diffusivity and  $\chi$  an arbitrary function.

2.a) The loading increments  $\delta \mathbf{A}$  represent perturbations of the form  $\delta \mathbf{A} \sim \mathbf{v} \wedge \mathbf{B}$ , with  $\mathbf{v}$  the velocity of an implicitly assumed plasma which flows upwards and expands (see Fig. 2), so that the loading process implements the action of the convective term in Eq. (4).

2.b) Bursts are localized diffusion processes, accompanied by energy release through current dissipation. Bursts implement the solution to the diffusive part of Eq. (4) in one time-step, with some characteristic simplifications, though.

3. Bursts occur there where the currents are large, and after a burst the local current is relaxed (Fig. 3).

4. An important innovation of the X-CA model is the direct use of the current in the instability criterion. With this modification, the X-CA directly implements Parker's (1993) flare scenario that an instability is triggered if the current  $J$  exceeds some threshold, since this implies that, through a current driven instability, the resistivity increases to anomalous values, and diffusion dominates over convection in the time evolution. The X-CA model incorporates thus the kinetic plasma physics which rules the behavior of the resistivity  $\eta$ , simulating the effect of occasionally appearing anomalous resistivities due to current instabilities.

5. The current-dissipation is spatially and temporally fragmented into a large number of practically independent, dispersed, and disconnected dissipation regions with the shape of current-surfaces, which vary in size and are spread over a considerable volume (Fig. 4). These current-surfaces do not grow in the course of time, but they multiply and are short-lived.

6. Important for future applications to particle acceleration is that the X-CA makes the electric fields explicitly

available as a function of time and space. The electric fields are short-lived and spatially distributed, and they spread and travel through space in the course of time (Fig. 5).

In conclusion, the X-CA model is a model for energy release through current dissipation, and it represents a realization of Parker's (1993) flare scenario. It allows interesting future developments, one of which is the introduction of particles into the system, which will allow to model the radiation signatures of the flaring plasma and the accelerated particles. This will put the comparison of CA models to observations on new grounds.

#### ACKNOWLEDGMENTS

This work was partly supported by the Greek General Secretariat of Research and Technology. The work of H. I. was partly supported by a grant of the Swiss National Science Foundation (NF grant No. 8220-046504).

#### REFERENCES

- Aschwanden, M.J., Montello, M., Dennis, B.R., Benz, A.O., 1995, *ApJ*, 440, 394
- Crosby, N.B., Aschwanden, M.J., Dennis, B.R., 1993, *Sol. Phys.*, 143, 275
- Crosby, N., Vilmer, N., Lund, N., Sunyaev, R., 1998, *A&A*, 334, 299
- Dennis, B.R., 1985, *Sol. Phys.*, 100, 465
- Einaudi, G., Velli, M., Politano, H., Pouquet, A., 1996, *ApJ*, 457, L13
- Galsgaard, K., 1996, *A&A*, 315, 312
- Georgoulis, M., Vlahos, L., 1996, *ApJ*, 469, L135
- Georgoulis, M., Vlahos, L., 1998, *A&A*, 336, 721
- Georgoulis, M., Velli, M., Einaudi, G., 1998, *ApJ*, 497, 957
- Georgoulis, M., Vilmer, N., Crosby, N. D., 2001, *A&A*, 367, 326
- Islaker, H., Anastasiadis, A., Vassiliadis, D., Vlahos, L., 1998, *A&A*, 335, 1085
- Islaker, H., Anastasiadis, A., Vlahos, L., 2000, *A&A*, 363, 1134
- Islaker, H., Anastasiadis, A., Vlahos, L., 2001, *A&A*, 377, 1068
- Lu, E.T., Hamilton, R.J., 1991, *ApJ*, 380, L89
- Lu, E.T., Hamilton, R.J., McTierman, J.M., Bromund, K.R., 1993, *ApJ*, 412, 841
- Parker, E.N., 1993, *ApJ*, 414, 389
- Pick, M., Klein, K.L., Trottet, G., 1990, *ApJS*, 73, 235
- Trottet, G., 1994, *Space Sci. Rev.*, 68, 149
- Vilmer, N., 1987, *Sol. Phys.*, 111, 207
- Vilmer, N., 1993, *Adv. Space Res.*, 13(9), 161
- Vilmer, N., Trottet, G., 1997, *Lecture Notes in Physics*, 483, 28
- Vlahos, L., Georgoulis, M., Kluiving, R., Paschos, P., 1995, *A&A*, 299, 897